

# Quantum Mpemba effect of Localization in the dissipative Mosaic model

J. W. Dong, H. F. Mu, M. Qin, and H. T. Cui\*

*School of Physics and Optoelectronic Engineering & Institute of Theoretical Physics, Ludong University, Yantai 264025, China*

(Dated: November 7, 2024)

The quantum Mpemba effect in open quantum systems has been extensively studied, but a comprehensive understanding of this phenomenon remains elusive. In this paper, we conduct an analytical investigation of the dissipative dynamics of single excitations in the Mosaic model. Surprisingly, we discover that the presence of asymptotic mobility edge, denoted as  $E_c^\infty$ , can lead to unique dissipation behavior, serving as a hallmark of quantum Mpemba effect. Specially, it is found that the energy level  $E_c^\infty$  exhibits a global periodicity in real configuration, which acts to inhibit dissipation in the system. Conversely, when the system deviates from  $E_c^\infty$ , the quasidisorder sets in, leading to increased dissipative effects due to the broken of periodicity. Furthermore, we find that the rate of dissipation is closely linked to the localization of the initial state. As a result, the quantum Mpemba effect can be observed clearly by a measure of localization.

## I. INTRODUCTION

Mpemba effect (ME) has a long history of research since its first experimental discovery in 1963[1]. In classical systems, ME shows that a thermal system at a high temperature  $T_h$  can be cooled down to equilibrium at a temperature faster than being at a low temperature  $T_l (< T_h)$  under identical condition. In the quantum realm, the quantum Mpemba effect (QME) characterizes the feature that a quantum system being far from equilibrium can relax to equilibrium faster than a system closer to equilibrium. Different methods are used to study QME, depending on the properties of system. In closed integrable systems, entanglement asymmetry is used to measure the restoration of symmetry in initially symmetry-broken states [2–9]. QME can also be observed in quantum simulations where systems starting with higher energy can relax faster than those starting with low energy[10].

Another intriguing situation arises in open quantum systems, where the dissipation can exhibit significant dependence on the initial condition [11–20]. For instance, it was found recently that the approach to stationary state in Markovian open quantum systems can be exponentially accelerated by performing an unitary transformation [12, 13]. This phenomena is known as strong ME, which has been verified experimentally [14]. Furthermore, QME can also be observed in open nonequilibrium quantum systems, where the system can relax to nonequilibrium steady states (NESS). By measuring the distance to NESS, QME can be identified by the intersection point at a finite time for distinct initial states [16, 17]. An interesting QME has been introduced recently, involving memory time scales induced by the non-Markovian dynamics of open quantum system [15]. Despite of observation of QME in various systems, a general understanding of it remains elusive.

In this paper, we introduce a new QME related to the localization in the Mosaic model coupled to bosonic

environment. The Mosaic model describes the one-dimensional quasiperiodic lattice system with the sinusoidal disorder appearing on the sites mediated by a unit cell composed of  $\kappa$  sublattices. The mobility edge can be emergent due to the competition between disorder and periodicity of unit cell. Crucially, the asymptotic mobility edge can be identified, independent of the strength of disorder. As will shown in the following discussion, the dissipative evolution of single excitation can demonstrate the significant correlation to the localization in initial state due to the presence of asymptotic mobility edge. Compared with the previous studies, the dissipative dynamics of excitation can be evaluated analytically in this case using Laplace transformation. The exact determination of the effective modes dominating the dynamics provides clear evidence for the QME of localization..

## II. MODEL AND METHOD

The Mosaic model coupled to a bosonic environment is depicted by the total Hamiltonian

$$H = H_s + H_b + H_{int}. \quad (1)$$

$H_s$  depicts the Mosaic model [21], written as

$$H_s = \sum_{n=1}^N \lambda \left( c_n^\dagger c_{n+1} + c_{n+1}^\dagger c_n \right) + \Delta_n c_n^\dagger c_n, \quad (2)$$
$$\Delta_n = \begin{cases} \Delta \cos(2\pi\beta n + \phi), & \text{if } n = j\kappa (j = 1, 2, \dots) \\ 0, & \text{otherwise.} \end{cases}$$

where  $N$  denotes the number of lattice and  $c_n (c_n^\dagger)$  is the annihilation (creation) operator of excitation at the  $n$ -th site.  $\lambda$  characterizes the hopping strength, which is assumed to be unitary in the following.  $\beta = (\sqrt{5} - 1)/2$  is the golden ratio, which is responsible for the quasiperiodicity in the system.  $\kappa$  is a positive integer, which denotes the size of unit cell. When  $\kappa = 1$ , the Mosaic model is reduced to the Aubry-André-Harper model [22, 23], for which the duality symmetry leads to the occurrence of localization-delocalization transition [22, 23]. While, for

\* cuiht01335@aliyun.com

$\kappa \neq 1$ , this symmetry is broken. Consequently, the mobility edge (ME)  $E_c$  can be determined exactly by [21]

$$a_k = \frac{1}{\sqrt{E_c^2 - 4}} \left[ \left( \frac{E_c + \sqrt{E_c^2 - 4}}{2} \right)^\kappa - \left( \frac{E_c - \sqrt{E_c^2 - 4}}{2} \right)^\kappa \right] \quad (3)$$

which separates the extended energy levels from localized ones. In Appendix I, the localization for all energy levels in Mosaic model is depicted in Fig. A1, measured by the inverse participation ratio. It is observed that as  $\Delta \rightarrow \infty$ ,  $E_c$  converges to an asymptotic value  $E_c^\infty$ , determined by solving  $a_k = 0$ . For instance, when  $\kappa = 2$ , we find that  $E_c = \pm \frac{2}{\Delta}$  and  $E_c^\infty = 0$ , while for  $\kappa = 3$ , we have  $E_c = \pm \sqrt{1 \pm 2/\Delta}$  and  $E_c^\infty = \pm 1$ . As will shown later, the energy level corresponding to  $E_c^\infty$  exhibits significant resilience to dissipation, compared to the other levels. Additionally, it is worth noting that the stability of  $E_c^\infty$  arises from the discrete translational invariance in the real configuration.

$H_b$  depicts the environment, written as

$$H_b = \sum_k \omega_k b_k^\dagger b_k, \quad (4)$$

where  $b_k$  ( $b_k^\dagger$ ) is the bosonic annihilation (creation) operator for mode  $k$ . The coupling between Mosaic model and its environment is depicted by

$$H_{int} = \sum_{k,n} \left( g_k b_k c_n^\dagger + g_k^* b_k^\dagger c_n \right) \quad (5)$$

where  $g_k$  are the coupling constants. The open dynamics of Mosaic model is determined by the spectral density

$$J(\omega) = \sum_k |g_k|^2 \delta(\omega - \omega_k). \quad (6)$$

For specification, we choose the Lorentzian spectral density [24] in the following calculation, which has the form

$$J(\omega) = \frac{\eta \omega_c^2}{\omega^2 + \omega_c}, \quad (7)$$

where  $\omega_c$  is the spectrum width and  $\eta$  is the coupling strength.  $\omega$  is confined to the interval  $(-\infty, +\infty)$ , allowing for an unbounded spectrum in the environment. This choice rules out the occurrence of discrete bound state [25, 26], which protects excitation from dissipating by creating an energy gap between the bound state and the spectrum in environment. Consequently, the excitation would be absorbed ultimately by environment, leading to a unique equilibrium in this scenario.

Since the absence of particle interaction in the Mosaic model, the study focuses on the dynamics for a single excitation at zero temperature in this paper. In this scenario, the state of system and environment can be written in a compact form

$$|\psi(t)\rangle = \left( \sum_{n=1}^N \alpha_n(t) c_n^\dagger + \sum_{k=1}^K \beta_k(t) b_k^\dagger \right) |0\rangle^{\otimes N} |0\rangle^{\otimes K}. \quad (8)$$

$|0\rangle$  is the vacuum state, and  $K$  denotes the number of frequency modes in environment. Substituting Eq. (8) into Schrödinger equation and solving first for  $\beta_k(t)$ , one can find an integrodifferential equation for  $\alpha_n(t)$ ,

$$i \frac{\partial}{\partial t} \alpha_n(t) = [\alpha_{n+1}(t) + \alpha_{n-1}(t)] + \Delta_n \alpha_n(t) - i \sum_{n=1}^N \int_0^t d\tau \alpha_n(\tau) f(t - \tau), \quad (9)$$

where  $i = \sqrt{-1}$  and

$$f(t - \tau) = \int_0^\infty d\omega J(\omega) e^{-i\omega(t-\tau)}. \quad (10)$$

is the memory kernel.

This equation can be solved both numerically and analytically. The exact numerical evaluation involves discretizing the evolution time equally and finding  $\alpha_n(t)$  through iteration. However, this method becomes so exhaustive for long evolution times. Alternatively, Laplace transformation is adopted to find the analytical expression of  $\alpha_n(t)$ , showing its asymptotic properties. By Laplace transformation

$$A_n(p) = \int_0^\infty dt e^{-pt} \alpha_n(t), \quad (11)$$

Eq. (9) can be rewritten as

$$i [p A_n(p) - \alpha_n(0)] = A_{n+1}(p) + A_n(p) + \Delta_n A_n(p) - i \int_{-\infty}^{+\infty} d\omega \frac{J(\omega)}{p + i\omega} \sum_m A_m(p) \quad (12)$$

which constitutes a linear system of equations for  $A_n(p)$  and thus can be solved by Cramer's rule. However, it is noted that the integral  $\int_{-\infty}^{+\infty} d\omega \frac{J(\omega)}{p + i\omega}$  becomes divergent when  $ip = \omega$ . This problem can be resolved by virtue of Sokhotski-Plemelj (SP) formula

$$\lim_{\epsilon \rightarrow 0} \frac{1}{x - x_0 - i\epsilon} = \text{P} \frac{1}{x - x_0} + i\pi \delta(x - x_0), \quad (13)$$

where P denotes the principle value. One thus gets

$$\lim_{\epsilon \rightarrow 0} \int_{-\infty}^{+\infty} d\omega \frac{J(\omega)}{\omega - ip - i\epsilon} = \text{P} \int_{-\infty}^{+\infty} d\omega \frac{J(\omega)}{\omega - ip} + i\pi J(ip).$$

For instance, one has as for the Lorentzian spectral density Eq. (7)

$$\text{P} \int_{-\infty}^{+\infty} d\omega \frac{J(\omega)}{\omega - z} = \frac{\eta \pi \omega_c}{i \omega_c + z},$$

in which  $ip = z$  is assumed for convenience.

To obtain  $\alpha_n(t)$ , inverse Laplace transformation defined as

$$a_n(t) = \frac{1}{2\pi i} \int_{s-i\infty}^{s+i\infty} dp A_n(p) e^{pt} \quad (14)$$

$z_i$	$\kappa = 2$	$\kappa = 3$
$z_1$	3.37164 - i 0.193387	3.125206 - i 0.243343
$z_2$	2.17811 - i 0.0654878	1.896475 - i 0.036575
$z_3$	1.77457 - i 0.00509817	1.477545 - i 0.002295
$z_4$	1.22702 - i 0.0119018	<u>1.0 - i <math>5.07 \times 10^{-17}</math></u>
$z_5$	0.594323 - i 0.00182872	0.774981 - i 0.004798
$z_6$	<u><math>1.06 \times 10^{-16}</math> - i <math>7.30 \times 10^{-17}</math></u>	-0.126563 - i 0.006496
$z_7$	-0.0912537 - i 0.00428128	-0.371380 - i 0.00004543
$z_8$	-0.963238 - i 0.00926696	<u>-1.0 - i <math>7.16 \times 10^{-17}</math></u>
$z_9$	-1.13057 - i 0.0016377	-1.13493 - i 0.67839
$z_{10}$	-1.13266 - i 0.608806	-1.227166 - i 0.0035706
$z_{11}$	-1.69034 - i 0.0030446	-1.930205 - i 0.00685497
$z_{12}$	-2.61258 - i 0.00225544	-2.573718 - i 0.0170292
$z_{13}$	-2.84288 - i 0.00960152	-2.787129 - i 0.000595899

Table I. The solved poles  $z$  by finding the zeros of the determinant of coefficient matrix in Eq. (12). The steady poles are highlighted by underline. For this evaluation,  $N = 12$ ,  $\Delta = 2$ ,  $\phi = 0$ ,  $\eta = 0.1$ , and  $\omega_c = 1$  are chosen.

is applied. Obviously,  $ip$  characterizes the effective mode, which determines the single-excitation dynamics. Eq. (14) can be evaluated by the residue theorem. For this purpose, one has to find poles of  $A_n(p)$  denoted as  $ip_i = z_i$ , which are also the zero points of the determinant of the coefficient matrix in Eq. (12). Formally, one can get

$$\alpha_n(t) \approx \sum_i c_{n,i} e^{-iz_i t}, \quad (15)$$

in which  $c_{n,i}$  corresponds to the residue of  $A_n(p)$  at  $z_i$ . It is obvious that the set of poles  $z_i$  consists of the dynamical modes, which determines the dissipation of excitation. Especially, the imaginary part of  $z_i$  gives rise to the rate of dissipation, which is responsible for QME observed in the recent works [12–14]. It is emphasized that the summation  $\sum_n \alpha_n^*(0) c_{n,i}$  cannot be considered as the probability on the mode  $z_i$  for initial condition  $\{\alpha_n(0)\}$  since the number of  $z_i$  is always larger than the dimension of Hilbert space in the system. Furthermore, it is found that  $\sum_n \alpha_n^*(0) c_{n,i}$  can be complex, and moreover the modulus may be larger than unit.

### III. DYNAMICAL MODE AND LOCALIZATION IN MOSAIC MODEL

With these preparations, we are ready to investigate the single-excitation dynamics in the Mosaic model. By setting the determinant of coefficient matrix to zero, one can derive an equation of degree  $N + 1$  for pole  $z$ . As an illustration, the solved poles are demonstrated for the case of  $\kappa = 2$  and  $\kappa = 3$  respectively in Table I with  $\Delta = 2$  and  $N = 12$ . For  $\kappa = 2$ , one has  $E_c = \pm 1$  and for  $\kappa = 3$ ,  $E_c = 0, \pm\sqrt{2}$ . It is worth noting that all the poles

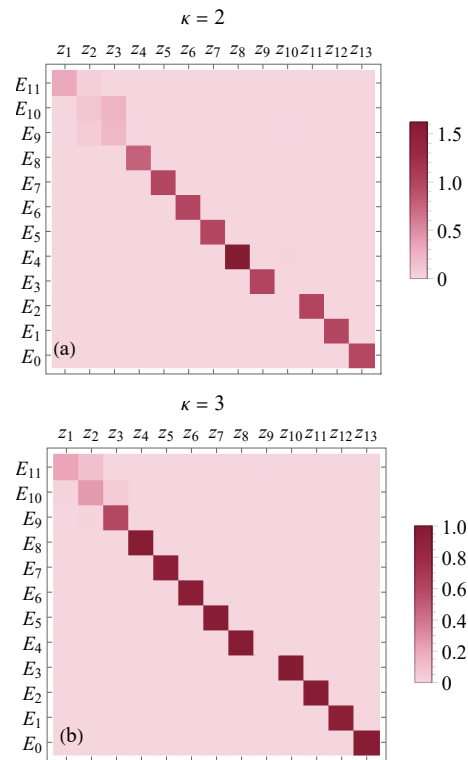


Figure 1. (Color online) The square modulus for the overlap between the energy level  $E_j$  ( $j = 0, 1, 2, \dots, 11$ ) (labeled in descending order) in the Mosaic model and the coefficient set  $\{c_{n,i}\}$  ( $n = 1, 2, \dots, N$ ) related to the initial state  $|E_j\rangle$ . For the plots, the parameters are chosen the same as those in Table I.

have negative imaginary parts, indicating the dissipative nature of excitation in the system. An interesting observation is that the imaginary part of pole is closed related to its corresponding real part. For instance, in the case of  $\kappa = 2$ , the pole  $z_6$  has a vanishing imaginary part, suggesting that this dynamics mode is resistant to dissipation. Interestingly, its real part tends towards zero, coinciding with the value of  $E_c^\infty$  for  $\kappa = 2$ . It should be emphasized that this coincidence is not occasional, as a similar pattern can be seen in the poles  $z_4$  and  $z_8$  for  $\kappa = 3$ , where their real parts match the value of  $E_c^\infty$  for  $\kappa = 3$ . Apart from the steady poles, the imaginary part of the other poles show a significant increase, indicating varying speeds of dissipation depending on the distance from the steady pole. This suggests that excitations may exhibit different rates of dissipation based on their proximity to the steady pole. Consequently, Quantum Master Equation (QME) phenomena can be readily observed under these conditions.

It is a natural assumption that the measure of "distance" would be related to the localization in Mosaic model. To confirm this point, the overlap between the energy level  $E_j$  ( $j = 0, 1, 2, \dots, 11$ ) in the Mosaic model and the corresponding coefficient set  $\{c_{n,i}\}$  ( $n = 1, 2, \dots, N$ ) for mode  $z_i$ , is shown in Fig. 1. According to Eq. (15),

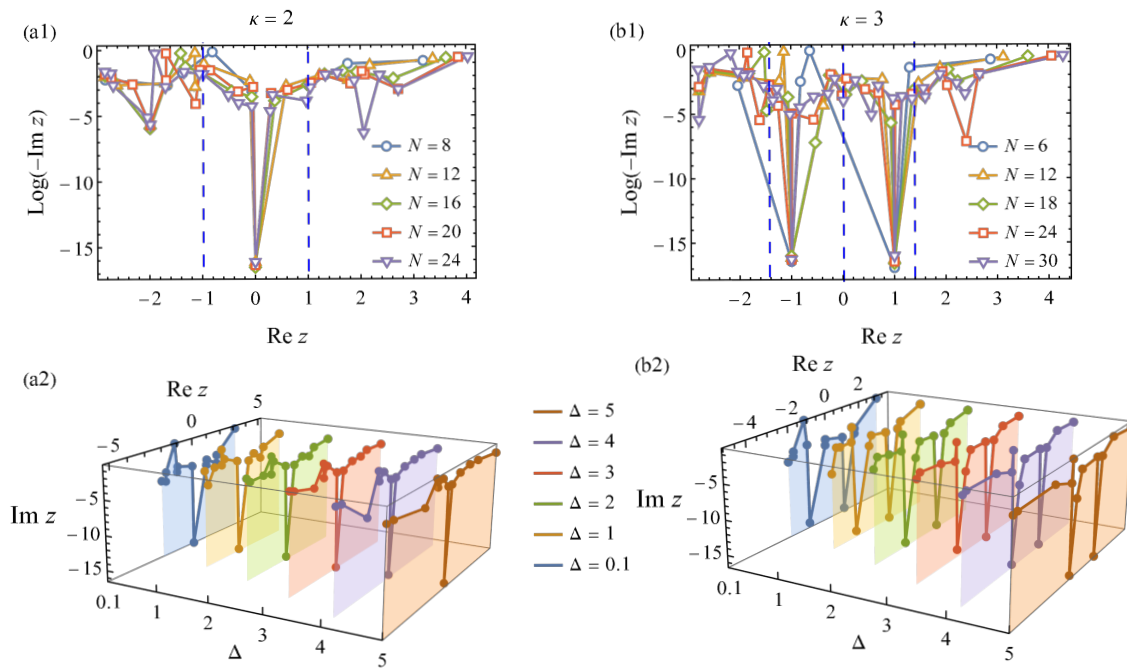


Figure 2. (Color online) The plots for the poles  $z_i$  with different  $\Delta$ s and  $N$ s. In panels (a1) and (b1),  $\Delta = 2$  is chosen. The blue-dashed lines labels the position of  $\text{Re } z = E_c$ . In panels (a2) and (b2),  $N = 12$  is chosen. The other parameters are the same as those in Table I.

this overlap actually characterizes the contribution of mode  $z_i$  to the survival probability of energy eigenstate in Mosaic model as initial state. As depicted in Fig. 1, the energy level  $E_j$  can display a significant overlap to the set  $\{c_{n,i}\}$  for a special mode  $z_i$ . While the overlap cannot be interpreted as the probability of initial state on the mode  $z_i$ , it does indicate the influence of dynamic mode  $z_i$  on the dissipative evolution of energy level. This suggests that a particular mode  $z_i$  would play a dominant role in the dissipation for a given level  $E_j$  as initial state. In this context, the mode  $z_i$  may be seen as the renormalization of  $E_j$ . Since the level  $E_j$ s exhibits distinct localizations due to the presence of mobility edge [21], the dissipation characterized by mode  $z_i$  may be seen as a consequence of localization in the energy level. Therefore, one could adopt the localization as a measure of the deviation of initial state from equilibrium. The dissipation leads to the system reaching equilibrium by releasing excitation into environment, ultimately causing the measure of localization to diminish.

Some comments should be made now. First as depicted in Fig. 2, the presence of steady poles  $z_6$  or  $z_{4(8)}$  is not influenced by the value of  $N$  and  $\Delta$ , indicating that it is a inherent characteristic of the Mosaic model. To understand the physical basis for the steady poles, we have explicitly calculated the energy levels  $E_6$  for  $\kappa = 2$  and  $E_{4(8)}$  for  $\kappa = 3$  since their close correspondence to the steady poles, as illustrated in Fig. 1. It is found that the eigenstates corresponding to  $E_6$  and  $E_{4(8)}$  exhibit a distinct periodicity in real configuration, which can be

expressed as

$$\begin{aligned}
 |E_6\rangle &= \frac{1}{\sqrt{6}} \left( c_1^\dagger - c_3^\dagger + c_5^\dagger - c_7^\dagger + c_9^\dagger - c_{11}^\dagger \right) |0\rangle \\
 |E_4\rangle &= \frac{1}{2\sqrt{2}} \left( c_1^\dagger + c_2^\dagger - c_4^\dagger - c_5^\dagger + c_7^\dagger + c_8^\dagger - c_{10}^\dagger - c_{11}^\dagger \right) |0\rangle \\
 |E_8\rangle &= \frac{1}{2\sqrt{2}} \left( c_1^\dagger - c_2^\dagger + c_4^\dagger - c_5^\dagger + c_7^\dagger - c_8^\dagger + c_{10}^\dagger - c_{11}^\dagger \right) |0\rangle.
 \end{aligned}$$

In  $|E_6\rangle$ , only the odd lattice sites can be occupied with a constant phase shift  $\pi$ . This results in a periodic variance by two lattice sites, known as 2-period. On the other hand, both  $E_4$  and  $E_8$  displays the periodic occupation in groups of three consecutive lattice sites, known as 3-period. The periodicity observed in these states is due to the periodic distribution of lattice sites with zero on-site potential, as described by  $\Delta_n$  in Eq. (2). This periodicity, along with the presence of quasidisorder, leads to the formation of a mobility edge. Thus, it is not surprising that the periodic eigenstate are able to withstand the influence of quasidisorder and remain stable even as the disorder strength approaches infinity, resulting in the mobility edge  $E_c^\infty$ . The stability of these periodic states is protected by the periodicity inherent in the Mosaic model. When this periodicity is disrupted, localization occurs, making the poles unstable against dissipation.

Secondly, there is always an additional pole, such as  $z_{10}$  for  $\kappa = 2$  and  $z_9$  for  $\kappa = 3$  in Table I, where the imaginary part is larger compared to the others. As demonstrated in Fig. 1, this special mode has a minimal impact to the survival probability of energy level  $E_j$  as initial state. In

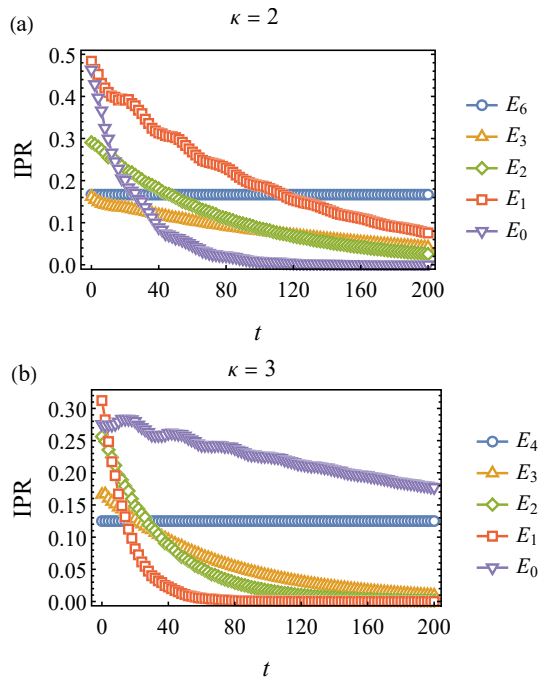


Figure 3. (Color online) The time evolution of IPR for four chosen initial states being the energy levels in the Mosaic model in the cases of  $\kappa = 2$  and  $\kappa = 3$  respectively. The parameters are chosen the same as those in Table I.

this meaning, this mode would serve to characterize the scenario of excitation embedding in environment, thus not affecting the dissipation of excitation in the system. Similarly, the pole with the highest real part also shows a finite imaginary part. This mode could be roughly considered as the renormalized highest excited state in Mosaic model, which decays very faster than the other energy levels.

Finally, it is observed in Figs. 2 that the imaginary parts of poles, excluding the additional poles, exhibit a regular variance with respect to the mobility edge  $E_c$ . For instance, focusing on the region  $|\text{Re}z_i| \leq 1$  in the case of  $\kappa = 2$ , the poles in this region generally have smaller imaginary parts globally compared to the other poles, as shown in Figs. 2 (a1). However, it also is noted that the poles near  $\text{Re}z_i = \pm 2$  can show the much smaller imaginary parts for a special  $N$ . Upon further calculation, it is found that their real parts are very closed to the eigenenergy of Mosaic model in this scenario. Thus, the phenomenon may be attributed to occasional resonance between the dynamical mode and the energy level of Mosaic model, and thus is nonuniversal. A similar trend can be observed in the case of  $\kappa = 3$ , as shown in Figs. 2 (b1).

#### IV. QUANTUM MPEMBA EFFECT FOR LOCALIZATION

The significant correlation between the dynamical mode and the localization in Mosaic model can give rise to unique dynamics of excitation. By inverse participation ratio (IPR) as a measure the localization defined by Eq. (A1), the time evolution of localization is plotted for initial states being the energy levels in Mosaic model in Fig. 3. From the observation in Table I and Fig. 1, it is evident that certain energy levels exhibit significant overlap with special poles, influencing the dissipative dynamics. As shown in Fig. 3, IPR shows varying rates of dissipation for different initial states, determined by the imaginary parts of the corresponding poles. As a result, the evolution paths intersect at certain times, indicating the occurrence of QME [12–14].

Finally, it is important to note that the system can be steady two different scenarios due to the existence of steady poles. One scenario is that when excitation is absorbed by environment, the system is in equilibrium and IPR tends to be zero, as shown in Figs. 3 (a) and (b) for  $E_0, E_1, E_2, E_3$ . The other is that when the system reaches a steady state, the excitation can remain in the system by a finite probability, and thus IPR can be a finite constant. As shown in Fig. 3 (a) for  $E_6$  and (b) for  $E_4$ , IPR remains constant as the energy levels coincide with the steady pole  $z_6$  for  $\kappa = 2$  and  $z_8$  for  $\kappa = 3$  respectively. It is worth noting that QME can be defined only if the initial state with distinct localization decays to the same equilibrium. The presence of steady poles indicates enhanced dissipation due to localization.

#### V. CONCLUSION

In conclusion, the single excitation dynamics in the Mosaic model coupled to the bosonic environment is studied analytically in this paper by determining the dynamical modes. It is found that the dynamical modes are closely tied to the energy levels in Mosaic model. Furthermore, due to the existence of robust asymptotic mobility edge, the dynamics of excitation displays the significant correlation to the localization in the Mosaic model. Specially, we observe that the asymptotic mobility edge  $E_c^\infty$  corresponds to a steady dynamical mode, which shows vanishing imaginary part and thus means dissipationless. The energy level  $E_c^\infty$  also exhibits a global periodicity in real configuration, determined by the spacial period in Mosaic model. Apart from  $E_c^\infty$ , the dynamical mode shows finite imaginary part, reflecting the dissipative dynamics. This suggests a relationship between the dissipative dynamics of excitation and the localization properties of the Mosaic model. By adopting IPR as a measure of localization, the paths of evolution for IPR can intersect at different times for various initial states, highlighting the localization-related QME.

It should be pointed out that mobility edge can emerge

by introducing the short-term [27] or long-term hopping [28] or by breaking the duality symmetry [29–32] in the Aubry-André-Haper model [22, 23]. In comparison to the Mosaic model, the mobility edges in these cases show generally dependence on the strength of quasidisordered on-site potential, and therefore the asymptotic mobility edge does not occur. Consequently, coupling to environment would change the mobility edge, leading to ambiguity in the correlation between localization and dissipation. Our investigation for the single excitation dynamics in the generalized Aubry-André-Haper model introduced in Ref. [30] has confirmed this hypothesis.

Finally, it is crucial for QME of localization that the extended energy level  $E_c^\infty$  can withstand dissipation and exhibit the periodicity related to the value of  $\kappa$  in the Mosaic model. In physics, the robustness of energy level  $E_c^\infty$  is a result of the homogeneous coupling for lattice to environment, as shown in Eq.(5), maintaining the global periodicity in Mosaic model invariant. This suggests that the asymptotic mobility edge may persist beyond the single-excitation subspace or in the presence of particle interaction. However, exploring multiple-excitation dissipative dynamics in interacting many-body systems poses a theoretical challenge that remains to be addressed in future research.

## ACKNOWLEDGEMENTS

H.T.C. acknowledges the support of Natural Science Foundation of Shandong Province under Grant No. ZR2021MA036. M.Q. acknowledges the support of NSFC under Grant No. 11805092 and Natural Science Foundation of Shandong Province under Grant No. ZR2018PA012.

## Appendix I. THE LOCALIZATION OF ENERGY LEVEL IN THE MOSAIC MODEL

In this appendix, a brief discussion about the localization in Mosaic model is presented. It is known that due to the existence of mobility edge, the energy levels in Mosaic model can exhibit unique localization characteristics. To quantify the localization, the inverse participation ratio

(IPR) is evaluated, defined as

$$\text{IPR} = \sum_n |\alpha_n|^4. \quad (\text{A1})$$

IPR reaches its minimum  $1/N$  when  $|\alpha_n|^2 = 1/N$  for all  $n$ , demonstrating a completely extended state. Conversely, the IPR reaches its maximum value of 1 when the excitation is localized on a specific site, indicating complete localization. As shown in Fig. A1, the energy level of the system can exhibit either localized or extended behavior depending on its position relative to the mobility edge. The coexistence of localized and extended state is a

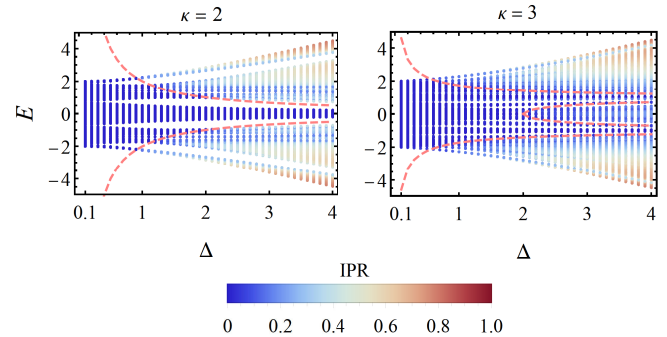


Figure A1. (Color online) The plot of IPR for all energy levels in Mosaic model in the cases of  $\kappa = 2$  and  $\kappa = 3$  respectively. The dashed-pink line characterizes the mobility edge, decided by Eq. (3). For the plots,  $N = 610$ ,  $\Delta = 2$  and  $\phi = 0$  are chosen.

typical feature for Mosaic model, leading to the complex dynamics in the system.

The presence of  $E_c^\infty$  in Mosaic model is a result of the periodicity, decided by the onsite potential  $\Delta_n$  in Eq. (2). It has been observed that  $E_c^\infty$  is one of the eigenvalues of  $H_s$  only when  $N/\kappa$  is even. In physics, the Mosaic model depicts a lattice system that showcases both disorder and invariant by discrete translation. It is obvious from definition of  $\Delta_n$  that the disorder presents only at the site  $n = j\kappa$ , while the discrete translation invariance happens for the other sites. The interplay between disorder and discrete translation invariance gives rise to the emergence of mobility edge.

- 
- [1] E. B. Mpemba and D. G. Osborne, Cool?, Phys. Educ. **4**, 172 (1969).
  - [2] F. Ares, S. Murciano, and P. Calabrese, Entanglement asymmetry as a probe of symmetry breaking, Nat. Commun. **14**, 2036 (2023).
  - [3] S. Murciano, F. Ares, I. Klich, and P. Calabrese, Entanglement asymmetry and quantum mpemba effect in the XY spin chain, J. Stat. Mech., 013103 (2024).
  - [4] F. Ares, S. Murciano, E. Vernier, and P. Calabrese, Lack of symmetry restoration after a quantum quench: An

entanglement asymmetry study, SciPost Phys. **15**, 089 (2023).

- [5] K. Chalas, F. Ares, C. Rylands, and P. Calabrese, Multiple crossing during dynamical symmetry restoration and implications for the quantum mpemba effect, arXiv: 2405.04436 (2024).
- [6] C. Rylands, K. Klobas, F. Ares, P. Calabrese, S. Murciano, and B. Bertini, Microscopic origin of the quantum mpemba effect in integrable systems, Phys. Rev. Lett. **133**, 010401 (2024).



- [7] Lata Kh. Joshi, J. Franke, A. Rath, F. Ares, S. Murciano, F. Kranzl, R. Blatt, P. Zoller, B. Vermersch, P. Calabrese, Christian F. Roos, and Manoj K. Joshi, Observing the Quantum Mpemba Effect in Quantum Simulations, *Phys. Rev. Lett.* **133**, 010402 (2024).
- [8] S. Liu, H.-K. Zhang, S. Yin, S.-X. Zhang, and H. Yao, Quantum Mpemba effects in many-body localization systems, arXiv: 2408.07750 (2024).
- [9] S. Liu, H.-K. Zhang, S. Yin, S.-X. Zhang, Symmetry restoration and quantum Mpemba effect in symmetric random circuits, *Phys. Rev. Lett.* **133**, 140405 (2024).
- [10] W.-X. Chang, S. Yin, S.-X. Zhang, and Z.-X. Li, Imaginary-time Mpemba effect in quantum many-body system, arXiv: 2409.06547 (2024).
- [11] Z. Lu and O. Raz, Nonequilibrium thermodynamics of the Markovian Mpemba effect and its inverse, *Proceedings of the National Academy of Sciences* **114**, 5083 (2017).
- [12] F. Carollo, A. Lasanta, and I. Lesanovsky, Exponentially accelerated approach to stationarity in markovian open quantum systems through the mpemba effect, *Phys. Rev. Lett.* **127**, 060401 (2021).
- [13] S. Kochsiek, F. Carollo, and I. Lesanovsky, Accelerating the approach of dissipative quantum spin system towards stationarity through global spin rotations, *Phys. Rev. A* **106**, 012207 (2022).
- [14] Jie Zhang, Gang Xia, Chun-Wang Wu, Ting Chen, Qian Zhang, Yi Xie, Wen-Bo Su, Wei Wu, Cheng-Wei Qiu, Ping-Xing Chen, Weibin Li, Hui Jing, and Yan-Li Zhou, Observation of quantum strong Mpemba effect, arXiv: 2401.15951 (2024).
- [15] D. J. Strachan, A. Purkayastha, and S. R. Clark, Non-Markovian quantum Mpemba effect, arXiv: 2402.05756 (2024).
- [16] A. Nava, adna R. Egger, Mpemba effect in open nonequilibrium quantum systems, arXiv: 2406.03521 (2024).
- [17] X. Wang and J. Wang, Mpemba effect in nonequilibrium open quantum system, arXiv:2401.14259 (2024)
- [18] A. K. Chatterjee, S. Takada, and H. Hayakawa, Quantum Mpemba Effect in a Quantum Dot with Reservoirs, *Phys. Rev. Lett.* **131**, 080402 (2023).
- [19] A. K. Chatterjee, S. Takada, and H. Hayakawa, Multiple quantum Mpemba effect: exceptional points and oscillations, *Phys. Rev. A* **110**, 022213 (2024).
- [20] X. Wang, J. Su and J. Wang, Mpemba meets quantum chaos: Anomalous relaxation and Mpemba crossings in dissipative Sachdev-Ye-Kitaev models, arXiv: 2410.06669 (2024).
- [21] Y.-P. Wang, X. Xia, L. Zhang, H.-P. Yao, S. Chen, J.-G. You, Q. Zhang and X.-J. Liu, One-dimensional quasiperiodic Mosaic Lattice with exact mobility edges, *Phys. Rev. Lett.* **125**, 196604 (2020).
- [22] S. Aubry and G. André, Analyticity Breaking and Anderson Localization in Incommensurate Lattices, *Ann. Isr. Phys. Soc.* **3**, 33 (1980);
- [23] P. G. Haper, Single Band Motion of Conduction Electrons in a Uniform Magnetic Field, *Proc. Phys. Soc. London Sect. A* **68**, 874 (1955)
- [24] B. Bellomo, R. Lo Franco, and G. Compagno, Non-Markovian Effects on the Dynamics of Entanglement, *Phys. Rev. Lett.* **99**, 160502 (2007).
- [25] E. Yablonovitch, Inhibited Spontaneous Emission in Solid-State Physics and Electrics, *Phys. Rev. Lett.* **58**, 2059-2062 (1987).
- [26] S. John and J. Wang, Quantum Electrodynamics near a Photonic Band Gap: Photon Bound States and Dressed Atoms, *Phys. Rev. Lett.* **64**, 2418-2421 (1990).
- [27] J. Biddle and S. Das Sarma, Predicted Mobility Edges in One-dimensional Incommensurate Optical lattices: An Exactly Solvable Model of Anderson Localization, *Phys. Rev. Lett.* **104**, 070601 (2010).
- [28] X. Deng, S. Ray, S. Sinha, G. V. Shlyapnikov, and L. Santos, One-Dimensional Quasicrystals with Power-Law Hopping, *Phys. Rev. Lett.* **123**, 025301 (2019).
- [29] S. Das Sarma, Song He, and X. C. Xie, Mobility Edge in a Model One-Dimensional Potential, *Phys. Rev. Lett.* **61**, 2144 (1988).
- [30] S. Ganeshan, J. H. Pixley, and S. Das Sarma, Nearest Neighbor Tight Binding Models with an Exact Mobility Edge in One Dimension, *Phys. Rev. Lett.* **114**, 146601 (2015).
- [31] X. Li, X.-P Li, and S. Das Sarma, Mobility edges in one-dimensional bichromatic incommensurate potentials, *Phys. Rev. B* **96**, 085119 (2017).
- [32] H. Yao, A. Khoudli, L. Bresque, and L. Sanchez-Palencia, Critical Behavior and Fractality in Shallow One-Dimensional Quasiperiodic Potentials, *Phys. Rev. Lett.* **123**, 070405 (2019).